

Metabolic programming of *Rhododendron chrysanthum* leaves following exposure to UVB irradiation

Xiaofu Zhou^A, Jie Lyu^B, Li Sun^C, Jiawei Dong^A and Hongwei Xu^{A,*} 

For full list of author affiliations and declarations see end of paper

***Correspondence to:**

Hongwei Xu
Faculty of Jilin Provincial Key Laboratory of Plant Spectral Regions Science and Green Production, Jilin Normal University, Siping 136000, China
Email: xuhongwei@jlnu.edu.cn

Handling Editor:

Suleyman Allakhverdiev

Received: 9 June 2020

Accepted: 7 August 2021

Published: 4 October 2021

Cite this:

Zhou X *et al.* (2021)
Functional Plant Biology, **48**(11), 1175–1185.
doi:[10.1071/FP20386](https://doi.org/10.1071/FP20386)

© 2021 The Author(s) (or their employer(s)). Published by CSIRO Publishing.

This is an open access article distributed under the Creative Commons Attribution-NonCommercial-NoDerivatives 4.0 International License ([CC BY-NC-ND](https://creativecommons.org/licenses/by-nc-nd/4.0/)).

OPEN ACCESS

ABSTRACT

Excessive UVB reaching the earth is a cause for concern. To decipher the mechanism concerning UVB resistance of plants, we studied the effects of UVB radiation on photosynthesis and metabolic profiling of *Rhododendron chrysanthum* Pall. by applying 2.3 W m⁻² of UVB radiation for 2 days. Results showed that maximum quantum yield of PSII (F_v/F_m) and effective quantum yield of PSII (ϕ_{PSII}) decreased by 7.95% and 8.36%, respectively, following UVB exposure. Twenty five known metabolites were identified as most important by two different methods, including univariate and multivariate statistical analyses. Treatment of *R. chrysanthum* with UVB increased the abundance of flavonoids, organic acids, and amino acids by 62%, 22%, and 5%, respectively. UVB irradiation also induced about 1.18-fold increase in 11 top-ranked metabolites identified: five organic acids (D-2,3-dihydroxypropanoic acid, maleic acid, glyceric acid, fumaric acid and suberic acid), four amino acids (L-norleucine, 3-oxoalanine, L-serine and glycine), and two fatty acids (pelargonic acid and myristoleic acid). In addition, UVB irradiation increased the intermediate products of arginine biosynthesis and the TCA cycle. Taken together, the accumulation of flavonoids, organic acids, amino acids and fatty acids, accompanied by enhancement of TCA cycle and arginine biosynthesis, may protect *R. chrysanthum* plants against UVB deleterious effects.

Keywords: amino acids, arginine biosynthesis, chlorophyll fluorescence, fatty acids, flavonoids, metabolic profile, organic acids, photosynthesis, *Rhododendron chrysanthum*, TCA cycle, UVB irradiation.

Introduction

Plants inevitably encounter unfavourable growth conditions due to their sessile nature. After environmental stresses exposure, plant metabolism is disturbed either because of downregulation of metabolic enzymes, shortage of substrate, increased demand for specific molecules, or a combination of these factors and many other reasons (Jan *et al.* 2018; Kaya *et al.* 2019; Rama and Vinutha 2019). Consequently, the plant rearranges the metabolic network to maintain essential metabolism and adopt a new steady-state to adapt to the current stress (Obata and Fernie 2012). The metabolic rearrangement is necessary to meet the demand for anti-stress agents, for example, compatible solutes, antioxidants and stress-responsive proteins (Jan *et al.* 2018; Kaya *et al.* 2019; Rama and Vinutha 2019).

It is now widely known that the increased influx of UVB (280–315 nm) irradiation is primarily due to stratospheric ozone depletion (Kusano *et al.* 2011). High UVB radiation levels cause macromolecules disruption, ROS production, inhibition of photosynthesis and growth reduction (Knox *et al.* 2019). Plants implement various strategies to combat the UVB stress conditions. From the standpoint of metabolomics, several reports documented that the metabolic rearrangement occurred in plants to minimise the adverse effects of UV-radiation-induced damage in plants (Casati *et al.* 2011; Dias *et al.* 2018, 2020). Among all the metabolites, three types of compounds are significant in terms of UVB stress tolerance: (1) ROS scavengers; (2) UVB-absorbing metabolites; and (3) compounds that protect against UVB stress. Plants synthesise various metabolites that help to

scavenge the excess ROS generated due to the UVB stress conditions (Ahmad *et al.* 2010, 2019; Kohli *et al.* 2019). These metabolites include phenolic compounds, flavonoids, squalene, carotenoids, etc. (Parida *et al.* 2018; Yadav *et al.* 2019; Dias *et al.* 2020). Phenolics like gallic acid, coumaric acid, vanillic acid and hydroxybenzoic acid, induced by UVB exposure, may be associated with the resistance of *Arabidopsis thaliana* L. to UVB irradiation (Yadav *et al.* 2019). The flavonoids, including flavonols and anthocyanins, are the primary UVB-absorbing metabolites and ROS scavenger role (Kim *et al.* 2018; Parida *et al.* 2018). Quercetin, kaempferol and kaempferol glycosides are the flavonoids associated with UVB tolerance in plants (Berli *et al.* 2010; Kusano *et al.* 2011; Demkura and Ballaré 2012; Emiliani *et al.* 2013; Fasano *et al.* 2014). The metabolites that also confer UVB protection include lipophilic metabolites, benzoic acid and glucopyranoside (Dias *et al.* 2018; Yadav *et al.* 2019; Dias *et al.* 2020). The concentrations of long-chain alkanes (palmitic acid, oleic acid and oleamide) increased during UVB irradiation in *Olea europaea* L. plants (Dias *et al.* 2018, 2020). In addition, soluble sugars, mannitol and myo-inositol also combat the UVB stress by providing energy for metabolic re-establishment (Dias *et al.* 2020).

Despite these vital roles of metabolic regulation under UVB irradiation, our understanding of this mechanism is still fragmented. *Rhododendron chrysanthum* Pall. is an ornamental plant with high medicinal value (Zhou *et al.* 2017). *Rhododendrons* have been used in Asian, North American and European traditional medicine mainly against inflammation, pain, skin ailments, common cold and gastrointestinal disorders (Popescu and Kopp 2013). As mentioned above, the literature investigation did not show any latest information about the effects of UVB irradiation on *R. chrysanthum*. Therefore, it is necessary to study the mechanism concerning UVB resistance of *R. chrysanthum* plants.

Exploring the mechanism concerning stress resistance requires an in-depth knowledge of plant biological processes that enable plants to survive in stressful environments, and this knowledge can be obtained from 'omic' studies (Abdelrahman *et al.* 2018). Metabolomics is the study of metabolism globally, thus representing the absolute physiological state (Rama and Vinutha 2019). Plant metabolomics has become a potent tool to study the metabolic and molecular mechanisms regulating stress responses of the plant (Hong *et al.* 2016; Xie *et al.* 2021). In addition, the chlorophyll (chl) fluorescence is a decisive parameter for assessing the properties of the photosynthetic apparatus, a major target of UVB (Machado *et al.* 2017; Lyu *et al.* 2019).

This study aimed to demonstrate the differential accumulation of metabolites in *R. chrysanthum* plants under UVB stress conditions and the involvement of those metabolites in different pathways concerning UVB tolerance in *R. chrysanthum*. To achieve this objective, we employed a gas chromatography time-of-flight mass spectrometry (GC-TOFMS) for the first time to identify metabolites

from the leaf tissue of well-irradiated and UVB-stressed *R. chrysanthum* plants.

Materials and methods

Plant materials and treatment

Rhododendron chrysanthum Pall. was collected at altitudes between 1300 m and 2650 m on the Changbai Mountain. After transport to the laboratory, the plants were maintained in an artificial climate room simulated alpine environment (Lyu *et al.* 2019). The plants were grown in an artificial climate room at 18°C (14-h light)/16°C (10-h dark) under white fluorescent light at 50 μmol (photon) $\text{m}^{-2} \text{s}^{-1}$, with 60% of relative humidity.

UVB stress was imposed on 8-month-old seedlings by adding UVB radiation supply for 8 h per day. A set of well-irradiated plants served as a control. Metabolic profiling and chl fluorescence were measured after 2 days of the UVB stress imposition. Artificial radiation of UVB (295–315 nm) and PAR (400–700 nm) used in the present study are the same as that described previously (Lyu *et al.* 2019). Briefly, seedlings of *R. chrysanthum* were exposed to artificial radiation of UVB and PAR in replicates ($n = 6$). A 295-nm long-pass filter (Edmund, Filter Long 2IN SQ, NJ, USA) was placed over the culture bottle in UVB treatment. A 400-nm long-pass filter (Edmund) was placed over the culture bottle in control. Based on the transmittance function of the long pass filters, the irradiances of UVB treatment and PAR effectively received by the samples were: 2.3 W m^{-2} UVB and 50 μmol (photons) $\text{m}^{-2} \text{s}^{-1}$ PAR, measured with UV rays intensity metre (Sentry Optronics Corp., ST-513, China) and light metre (TES Electrical Electronic Corp., TES-1339 Light Meter Pro., China), respectively.

chl fluorescence measurements

chl fluorescence was measured as described previously (Lyu *et al.* 2019). Induction curves were obtained by using the Maxi version of an IMAGING PAM M-series (Walz, Effeltrich, Germany). The dark period of the samples was set for 20 min before measurements. Quantum efficiencies were calculated as follows: (1) maximum quantum yield of PSII (F_v/F_m); and effective quantum yield of PSII (ϕ_{PSII}). The equation was as follows: $F_v/F_m = (F_m - F_o)/F_m$, $\phi_{\text{PSII}} = (F'_m - F)/F'_m$, where the meaning of each parameter was given in the abbreviation section of this article.

Sample preparation

Plant samples with six biological repetitions were frozen in liquid nitrogen. Each group had six biological repetitions (e.g. six independent individuals) for screening statistically significantly differentiated metabolites among groups. The

untargeted metabolomics profiling was performed on the XploreMET platform (ver. 3.0, Metabo-Profile, Shanghai, China). The sample preparation procedures and the instrument settings are the same as those described previously (Qiu *et al.* 2014; Tang *et al.* 2020). Briefly, after derivatisation, each sample was analysed via GC-TOFMS system (Pegasus HT, Leco, USA) with gas chromatography (7890B, Agilent, USA) and a sample MPS2 with dual heads (Gerstel, Muehlheim, Germany). More details were provided in the Supplementary file, available at the journal website.

Metabolite annotation

Metabolite annotation was carried out by comparing the retention indices and mass spectral data with those in

the JiaLib metabolite database using the XploreMET software (ver. 3.0, Metabo-Profile). The peak area given here was relatively quantified data obtained by integrating the chromatographic peak for each metabolite.

Metabolic pathway enrichment analysis and ratio generation

The metabolic pathway enrichment and the critical metabolic networks determination were performed using a proprietary hypergeometric algorithm of the XploreMET software (ver. 3.0, Metabo-Profile). A P -value < 0.05 was regarded as significantly different, and the importance of the metabolic pathway was used to evaluate the impact value (Tang *et al.* 2020).

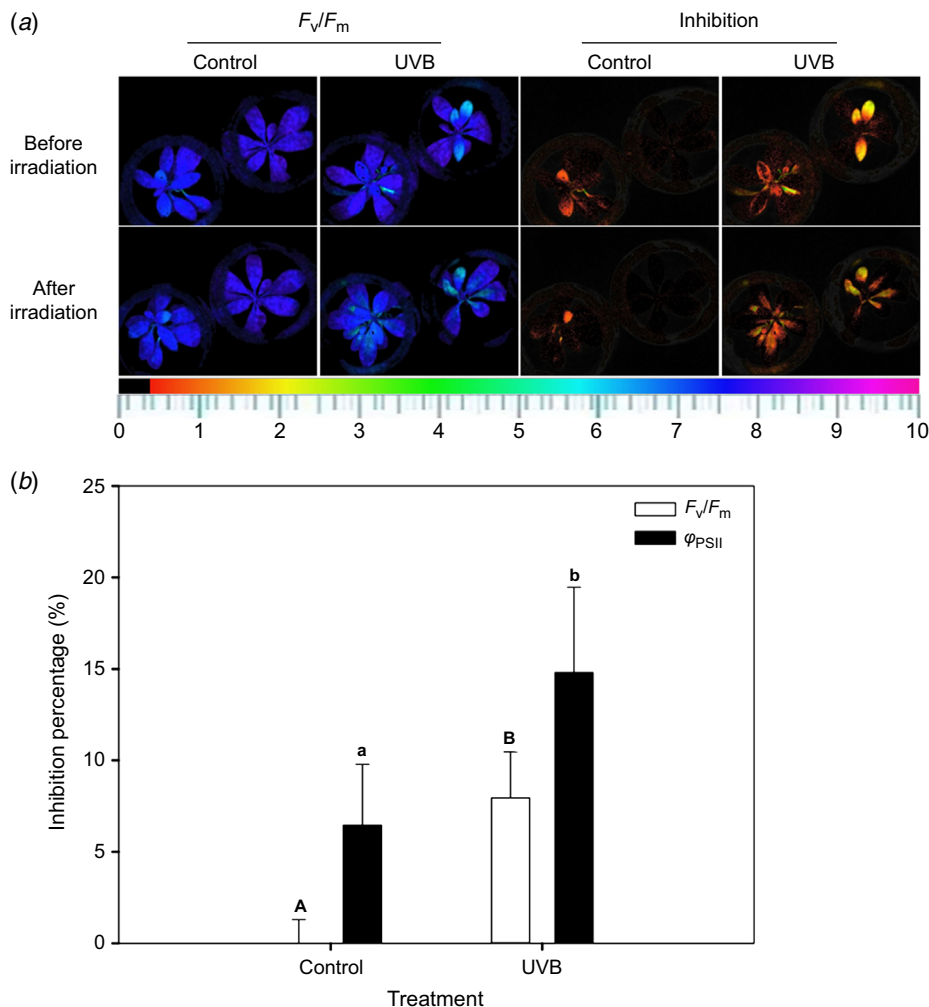


Fig. 1. Change in chlorophyll fluorescence in control and UVB-treated *R. chrysanthum* leaves. (a) Images of photosynthetic performance (F_v/F_m and inhibition). (b) Inhibition percentage of maximum quantum yield (F_v/F_m) and that of effective quantum yield (ϕ_{PSII}). The difference between absolute values obtained before and after treatment divided by the absolute value obtained before treatment is the inhibition percentage. Data are the means of six biological repetitions (\pm s.d.). Means labelled with the same letter did not significantly differ at $P < 0.05$ according to LSD.

The new feature of XploreMet 3.0 provides the metabolite ratios with biological significance. The ratios of the two adjacent metabolites from the specific metabolic relation network (KEGG) were calculated. The relationship of metabolite connectivity can be used for indicating metabolite enzyme activity. The ratio >1 means the enhanced enzyme activity, while the ratio <1 denotes inhibited enzyme activity (Rostami-Hodjegan et al. 1996, 1999).

Statistical analysis

One-way ANOVA followed by the least significant difference (LSD) as a *post hoc* test was performed using SPSS 16.0 (NY, USA) to test the single effects of control and treatment. In the results, letters were used to identify the levels of significance. The figures were prepared with Sigmaplot 12.5 (Systa Software Inc, Chicago, IL, USA).

Both single-dimensional method (*t*-test) and multi-dimensional method (OPLS-DA) were used to screen differential metabolites among groups. The single-dimensional method screens differences based on the distribution of a single variable in different groups. OPLS-DA's VIP focuses on screening features from the overall contribution of the variable to the model, and the selected variable is more vital in the interpretation ability of the *y* variable (Blasco et al. 2015). Therefore, using a multi-dimensional method, we can sort out the significant variables that are useless by themselves but valid together with others (Guyon and Elisseeff 2003).

Consequently, we showed the results obtained from both single-dimensional and multi-dimensional analysis so that readers can have a more comprehensive understanding of the differences of various metabolites.

A Z-score heat map was performed for the data visualisation of overall relationships. Fold change was calculated by the ratio of the mean between pairwise comparisons. A calculated fold change of 1.5 or a *P*-value of 0.05 was chosen for statistical significance. Statistical algorithms were adapted from the widely used statistical analysis software packages in R studio (<http://cran.r-project.org/>).

Results

Differential photosynthetic performance upon UVB exposure

Photosynthetic performance, such as F_v/F_m and ϕ_{PSII} , was compared to observe the effect of UVB irradiation on *R. chrysanthum*. chl fluorescence was measured using an IMAGING PAM. Results showed that both F_v/F_m and ϕ_{PSII} were significantly decreased after UVB irradiation, reducing by 7.95% and 8.36%, respectively (Fig. 1). No statistical difference was observed in the chl content, total chl or chl *a/b*, and in carotenoids content (data not shown).

Our previous study has shown that the inhibitory effects of UVB were dose-dependent, and the range of photosynthetic

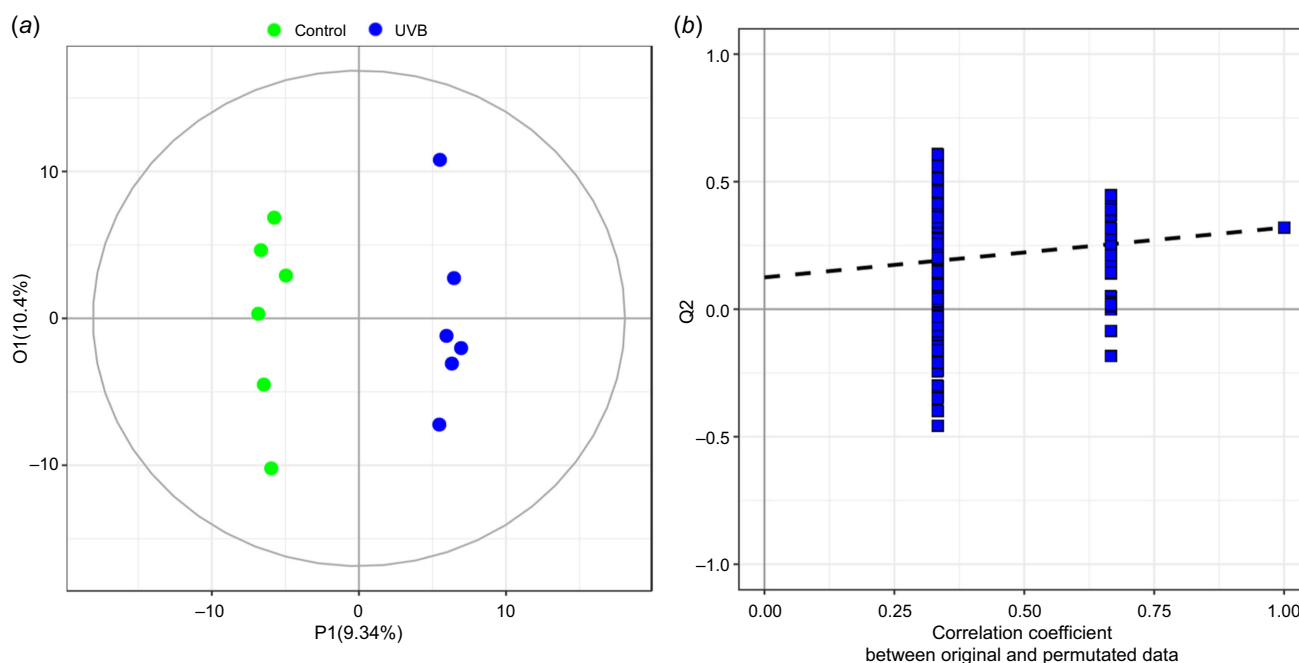


Fig. 2. Visualisation of overall metabolite profile difference in control and UVB-treated *R. chrysanthum* leaves. (a) OPLS-DA discriminate score plot IP + IO; R2Y = 0.991, Q2Y = 0.32. (b) 1000 permutation test intercept of Q2 in the y-axis is 0.125. Each group had six biological repetitions.

capacity in *R. chrysanthum* is ranked as follows: 48 h of UVB dose < *R. chrysanthum* plant < 72 h of UVB dose (Lyu *et al.* 2019). Therefore, a 48 h fixed time was chosen to test the UVB radiation effect on *R. chrysanthum* in this study.

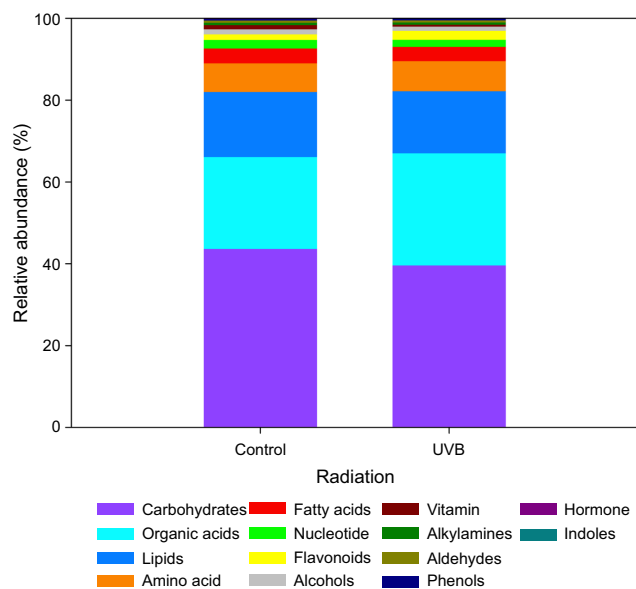


Fig. 3. Relative contribution of 14 classes of metabolites in control and UVB-treated *R. chrysanthum* leaves.

Metabolite profiling

A non-targeted GC-TOFMS approach was employed for the first time to determine the differential metabolites from the leaves of control and UVB-treated *R. chrysanthum* plants.

The metabolomics approach in this study detected 404 peaks, of which 204 were identified as known metabolites (40 including metabolite ratios), and the remaining peaks were unknown metabolites. Metabolites were highly measurable and reproducible among the six analysed biological replications under the two different conditions. The identified metabolites belong to the 14 classes – amino acids, organic acids, carbohydrates, fatty acids, nucleotides, lipids, flavonoids, alcohols, vitamins, alkylamines, aldehydes, phenols, hormone and indoles.

Metabolic profiles of the individuals from the two conditions (UVB and control) were further differentiated using the OPLS-DA model (Fig. 2). The first OPLS component (PC1) explained 10.4% of the total variation, whereas the second component (PC2) explained 9.34% variation across the data set (Fig. 2a). Two distinct groups associated with the UVB and control samples distinguished metabolite accumulation under two conditions (Fig. 2a). Permutation testing was performed to validate the classification model (Fig. 2b). A significance threshold of 0.4 is generally accepted for Q²Ycum. The model has Q²Y = 0.125, indicating a valid model (Fig. 2b).

Table 1. The differential metabolites of *R. chrysanthum* between control and UVB treatment, obtained from univariate statistical analysis.

Class	Name	KEGG ID	P-value	FC
Amino acid	L-Serine	C00065	0.058	3.019
	L-Norleucine	C01933	0.063	1.285
	Ratio of pyruvic acid/L-alanine	C00022/C00041	0.077	1.683
	Ratio of pyruvic acid/L-serine	C00022/C00065	0.08	0.439
	L-Alanine	C00041	0.08	0.538
	Ketoleucine	C00233	0.08	0.835
	3-Oxoalanine	NA	0.09	1.183
Carbohydrates	Galactonic acid	C00880	0.052	0.827
Fatty acids	Myristoleic acid ★	C08322	1.20E-02	1.586
Lipids	1-Linoleoyl- <i>sn</i> -monoglyceride ★	NA	3.80E-02	0.781
	1-(9Z-octadecenoyl)- <i>sn</i> -glycerol	NA	0.065	0.520
Nucleotide	Ratio of uridine/cytidine	C00299/C00475	0.083	5.046
Organic acids	Maleic acid ★	C01384	1.40E-02	1.839
	D-2,3-Dihydroxypropanoic acid ★	NA	3.80E-02	1.825
	Fumaric acid ★	C00122	3.60E-02	1.568
	Glyceric acid	C00258	0.088	1.583
	Quinic acid	C06746	0.091	0.432
	Suberic acid	C08278	0.098	2.411

Note: P-value < 0.05 was considered significant, and fold change (FC) < 1 indicates that the metabolite had significantly decreased, while fold change (FC) > 1 indicates that the metabolite had significantly increased. Fold change (FC) values were calculated by dividing metabolite concentration in UVB by that in control.

★ represents differentially expressed metabolites in control and UVB-treated plants.

The effect of UVB irradiation on metabolic arrangement becomes evident from the differential contribution of metabolites in *R. chrysanthum* plants under control and UVB irradiation (Fig. 3). Among the 14 classes of metabolites identified, carbohydrates, organic acids and lipids were predominant (15–45%) in the two samples examined (Fig. 3). Percent flavonoids, organic acids and amino acids showed higher values in UVB-irradiated leaves, increasing by 62%, 22% and 5%, respectively. On the contrary, percent lipids, fatty acids, carbohydrates and nucleotides showed lower values in UVB treatment, decreasing by 4%, 5%, 9% and 16%, respectively.

To demonstrate the important metabolites responsive to the UVB irradiation, univariate and multivariate statistical analyses, namely student *t*-test and OPLS-DA, were performed (Tables 1 and 2). The two methods showed quite similar results, identifying the same metabolites. UVB irradiation caused about 1.18-fold increase in 11 top-ranked metabolites identified: five organic acids (D-2,3-dihydroxypropanoic acid, maleic acid, glyceric acid, fumaric acid and suberic acid), four

amino acids (L-norleucine, 3-oxoalanine, L-serine and glycine), and two fatty acids (pelargonic acid and myristoleic acid) (Fig. 4). On the contrary, UVB irradiation led to a more than 0.43-fold decrease in six top-ranked metabolites identified. The decline of UVB-induced metabolites was in the order ketoleucine > galactonic acid > 1-linoleoyl-*sn*-monoglyceride > L-alanine > 1-(9Z-octadecenoyl)-*sn*-glycerol > quinic acid (Table 1). These results indicate that organic acids, amino acids, and fatty acids may be related to the UVB defence in *R. chrysanthum*.

Metabolic pathway analysis

Metabolic Pathway Enrichment Analysis (MPEA) was carried out to sort the metabolic pathways by mathematical algorithms according to the *P*-value involved. The metabolic pathways involved are shown in Fig. 5. The right side of the dotted line represents the metabolic pathway with *P* < 0.05. The redder the colour is, the more significant the *P*-value.

Table 2. The differential metabolites of *R. chrysanthum* between control and UVB treatment, obtained from multivariate statistics.

Class	Name	HMDB ID	KEGG ID	VIP	<i>P</i> -value	Correlation coefficients
Amino acid	L-Serine ▲	HMDB00187	C00065	2	3.90E–02	0.6
	L-Norleucine	HMDB01645	C01933	1.9	0.052	0.57
	Ratio of pyruvic acid/L-serine	HMDB00243/HMDB00187	C00022/C00065	1.8	0.059	–0.56
	Ketoleucine	HMDB00695	C00233	1.8	0.059	–0.56
	5-Hydroxylysine	HMDB00450	C16741	1.8	0.063	–0.55
	3-Oxoalanine	HMDB11602	NA	1.8	0.064	0.55
	Ratio of pyruvic acid/L-alanine	HMDB00243/HMDB00161	C00022/C00041	1.7	0.081	0.52
	Glycine	HMDB00123	C00037	1.7	0.088	0.51
	L-Alpha-aminobutyric acid	HMDB00452	C02356	1.7	0.091	–0.51
	L-Alanine	HMDB00161	C00041	1.6	0.098	–0.5
	Carbohydrates	Galactonic acid ▲	HMDB00565	C00880	2	3.00E–02
D-Threitol		HMDB04136	C16884	1.7	0.09	–0.51
Fatty acids	Myristoleic acid ▲	HMDB02000	C08322	2.2	1.60E–02	0.68
	Pelargonic acid	HMDB00847	C01601	1.7	0.078	0.53
	Dodecanoic acid	HMDB00638	C02679	1.7	0.084	–0.52
Lipids	1-Linoleoyl- <i>sn</i> -monoglyceride ▲	HMDB11568	NA	2.2	1.80E–02	–0.67
	1-(9Z-Octadecenoyl)- <i>sn</i> -glycerol	HMDB11567	NA	1.9	0.055	–0.57
Nucleotide	Ratio of uridine/cytidine	HMDB00296/HMDB00089	C00299/C00475	1.8	0.072	0.54
	Inosine	HMDB00195	C00294	1.7	0.092	–0.51
Organic acids	Maleic acid ▲	HMDB00176	C01384	2.3	1.00E–02	0.71
	D-2,3-Dihydroxypropanoic acid ▲	HMDB31818	NA	2.1	2.80E–02	0.63
	Fumaric acid ▲	HMDB00134	C00122	2.1	2.40E–02	0.64
	Glyceric acid	HMDB00139	C00258	1.7	0.086	0.52

Note: HMDB ID, Human Metabolome Database ID. Correlation coefficients were obtained via correlation analysis between score values of samples of the OPLS-DA model and variable X (peak area of a certain metabolite in all samples), representing the reliability of a specified metabolite. *P*-value < 0.05 was considered significant, and correlation coefficients < 0 indicates that the metabolite had significantly decreased, while correlation coefficients > 0 indicates that the metabolite had significantly increased.

▲ represents differentially expressed metabolites in control and UVB-treated plants.

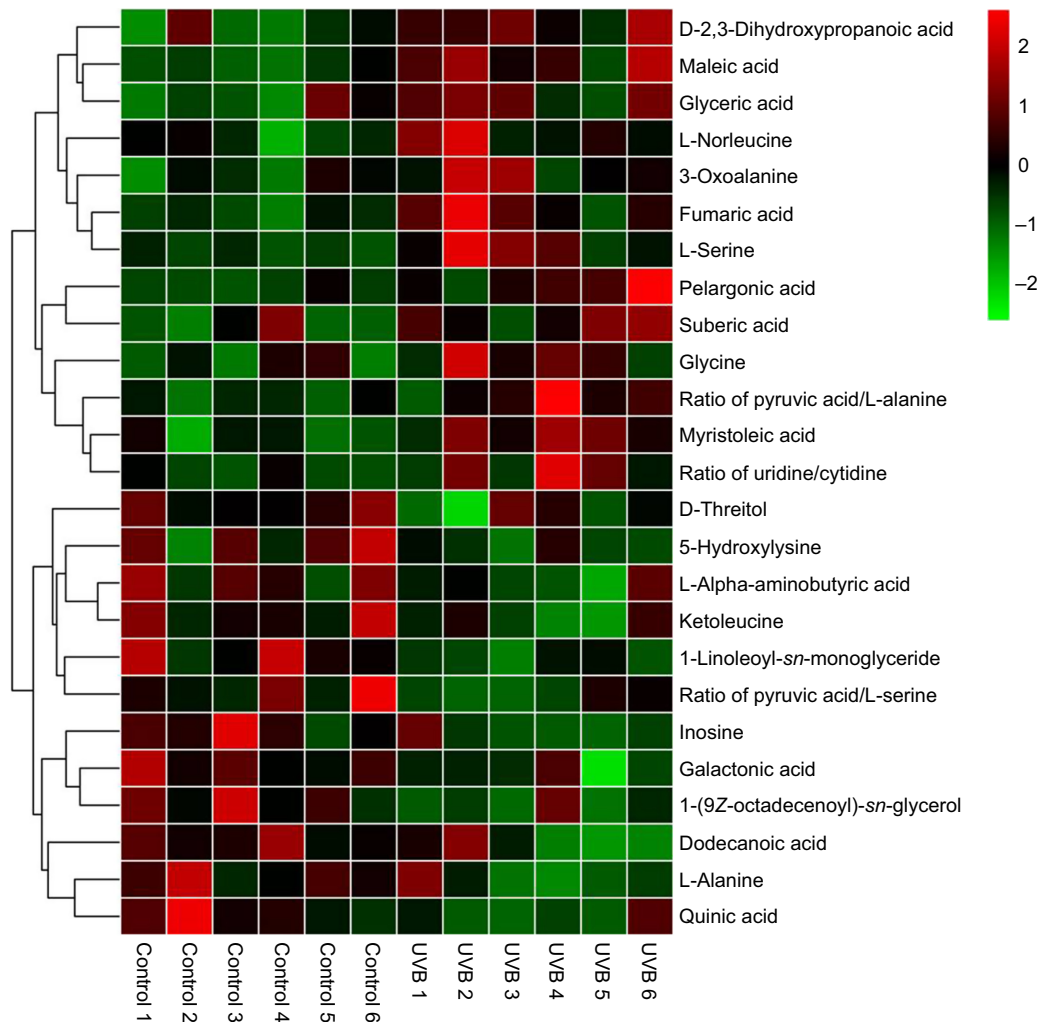


Fig. 4. Z-score heatmap illustrating the levels of differential metabolites in control and UVB-treated *R. chrysanthum* leaves. Data are the values of six biological repetitions of each group.

Thus, arginine biosynthesis needs to be focused on by observing UVB-dependent regulatory process, followed by the citrate cycle and pyruvate metabolism (Fig. 5; Figs S1–S3).

The most considerable difference between control and UVB-irradiated plants was fumaric acid content, indicating that UVB may enhance the activity of argininosuccinase (EC 4.3.2.1) in arginine biosynthesis (Fig. S1). The ratio of pyruvic acid/L-alanine denotes the ratio of product to reactant in arginine biosynthesis and/or alanine, aspartate, and glutamate metabolism (Figs S4 and S5). UVB irradiation markedly increased the ratio of pyruvic acid/L-alanine, indicating that their corresponding enzyme activity (L-alanine: 2-oxoglutarate aminotransferase, EC 2.6.1.2) may be enhanced by UVB irradiation (Fig. 6; Figs S4 and S5). UVB elevated the ratio of uridine/cytidine in pyrimidine metabolism (Fig. 6; Fig. S6). This indicates that UVB irradiation may enhance the activity of cytidine aminohydrolase (EC 3.5.4.5). In contrast, the ratio of pyruvic acid/L-serine was decreased

after UVB exposure. This suggests that UVB irradiation may inhibit the activities of L-serine ammonia-lyase (EC 4.3.1.17) and/or threonine ammonia-lyase (EC 4.3.1.19) in glycine, serine and threonine metabolism and/or in cysteine and methionine metabolism (Fig. 6; Figs S7 and S8).

Discussion

Metabolites related to enzyme activity under UVB irradiation

Several studies demonstrated that UVB could affect corresponding molecules either directly or by ROS generated during UVB irradiation (Kreslavski *et al.* 2018). To cope with UVB irradiation, the plant must develop a specific tolerance mechanism. Plants respond to UVB irradiation via the development of protective structures and molecules. The former

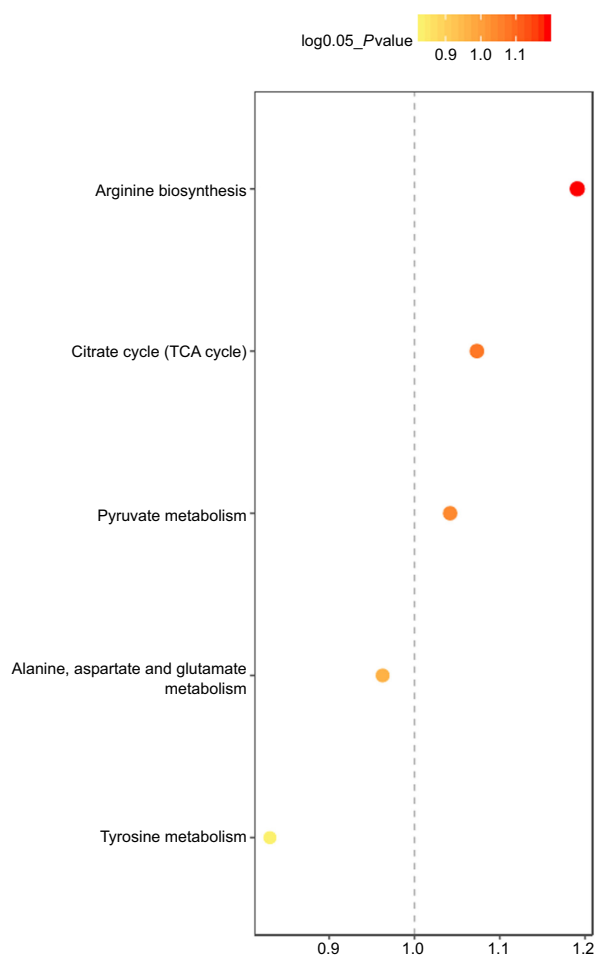


Fig. 5. Overview of pathway analyses involved in elevated levels of fumaric acid in *R. chrysanthum* in response to UVB irradiation. The right side of the dotted line represents the metabolic pathway with $P < 0.05$. The redder the colour is, the more significant the P -value.

involves hairs, waxes and other cellular modifications to provide an optical barrier, while the latter includes the synthesis of antioxidative enzymes and increased contents of protective compounds (Hamid *et al.* 2018; Takshak and Agrawal 2019). A recent report has suggested that tailoring enzymes that catalyse the last step of metabolite synthesis generally make a more significant contribution to the variation of metabolite abundance than early pathway enzymes (Peng *et al.* 2017). Our results showed that UVB irradiation significantly increased the accumulation of flavonoids, organic acids, amino acids and fatty acids, probably because the activities of tailoring enzymes that catalyse the final step of their biosynthesis varied with treatment. With this in mind, our ongoing research is characterising the tailoring enzymes, thereby helping understand the plant's defence mechanism against UVB radiation. This will be demonstrated in our future proteomic study.

In this work, UVB irradiation may affect the activities of five enzymes, including argininosuccinase, L-alanine:

2-oxoglutarate aminotransferase, cytidine aminohydrolase, L-serine ammonia-lyase and threonine ammonia-lyase (Fig. 6). However, the direct enzyme activity should be measured directly using the biological assays (i.e. ELISA). The next challenge is to characterise the enzymes involved in these pathways, through which the observed changes in metabolic pathways can be linked to the underlying genetic alterations.

Metabolites related to ROS detoxification under UVB irradiation

Of all the plant secondary metabolites reported, the metabolites of the phenylpropanoid pathway, the phenolics, have been the most widely reported to act as antioxidants (Kasote *et al.* 2015; Takshak and Agrawal 2019) since this pathway is universal in plants. Numerous phenylpropanoid pathway compounds have been reported to act as antioxidants, including flavonoids, phenolic acids, stilbenes and anthocyanins (Takshak and Agrawal 2019). Here, we showed that the abundance of the flavonoids was increased by 62% after UVB exposure. This may reflect that the abundance of the flavonoids appears to be related to UVB protection. Peng *et al.* (2017) concluded that the abundance of the flavone *O*-glucosides might be responsible for adaptation to UVB irradiance. Plants under UV-B had an increased total flavonoid content, as Hamid *et al.* (2020) found in *Cenchrus ciliaris* L., because UV-B radiation led to synthesis of key enzymes of the phenylpropanoid pathway.

In this study, UVB irradiation had also considerably increased the accumulation of organic acids, including D-2,3-dihydroxypropanoic acid, maleic acid and fumaric acid. Consistent with this, the increased accumulation of organic acids (i.e. D-2,3-dihydroxypropanoic acid, and maleic acid) under UVB irradiation was reported previously in high-altitude (2000–3400 m) maize (*Zea mays* L.) leaves (Casati *et al.* 2011). Organic acids play an important role in osmoregulation, ROS detoxification, and intracellular pH level adjustment (Farooq *et al.* 2009a, 2009b). Taken together, this could explain why both organic acids and flavonoids showed maximum increases in plants after UVB exposure.

Metabolites related to osmotic regulation under UVB irradiation

An increase in unsaturated/saturated fatty acids is a prerequisite for membrane rigidity (Hugly *et al.* 1989; Kramer *et al.* 1991). UVB irradiation enhanced total unsaturated fatty acids enhanced by 112% in our experiments but reduced saturated fatty acids by 6.24%. Thus, the unsaturated/saturated fatty acids ratio increased to 11% in *R. chrysanthum* exposed to UVB (Table 3). This implies that the rigidity of the cell membrane altered by UVB irradiation could accelerate the leakage of cell content in *R. chrysanthum*. The organic acids could alleviate it since they play an essential role in maintaining osmotic pressure (Farooq *et al.* 2009a, 2009b).

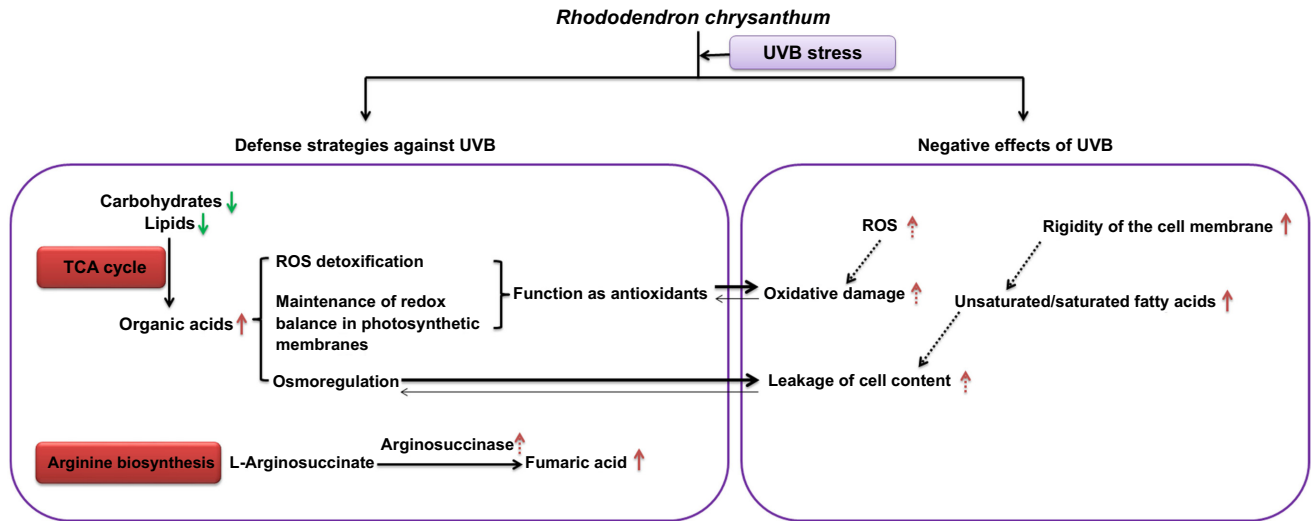


Fig. 6. The metabolic changes of *R. chrysanthum* in response to UVB stress. The red arrow represents upregulation. The green indicates downregulation. Two-way arrows represent mutual resistance (the thicker the arrow line, the greater the force). The box filled with red background represents enhancement. The dotted line represents speculation.

Table 3. Changes in fatty acid content in *R. chrysanthum* subjected to UVB radiation.

Fatty acids	Control	UVB	% increase
Unsaturated			
Palmitoleic acid	295.26	363.73	23.19
Linoleic acid	9310.90	8620.62	-7.41
Oleic acid	43.99	52.04	18.31
Elaidic acid	18 735.93	19 521.8	4.19
Docosahexaenoic acid	105.95	225.18	112.54
Myristoleic acid	1098.09	1966.60	79.09*
Total	29 590.11	30 749.96	3.92
Saturated			
Caproic acid	53.25	46.42	-12.82
Pelargonic acid	10.97	46.02	319.41
Dodecanoic acid	2068.91	1142.33	-44.79
Myristic acid	794.69	1207.65	51.96
Palmitic acid	1307.52	1209.12	-7.53
Heptadecanoic acid	539.46	487.69	-9.60
Arachidic acid	1538.81	1334.38	-13.29
Behenic acid	18 135.98	17 451.42	-3.77
Total	24 449.59	22 925.04	-6.24
Unsat./satur.	1.21	1.34	10.83

Note: The given values of fatty acids denote peak areas. Data are the means of six biological repetitions.

*, $P < 0.05$.

An increase in unsaturated/saturated fatty acids with UVB irradiation was probably due to the accumulation of unsaturated fatty acids, especially myristoleic acid. The content

of myristoleic acid in mangrove (*Rhizophora apiculata* Blume) was increased under high UVB irradiances (doses equivalent to 30–40% ozone depletion) (Moorthy and Kathiresan 1998). Except for Moorthy and Kathiresan (1998), no previous study has reported the presence of myristoleic acid in any plant subjected to UVB radiation.

Metabolites related to photosynthesis under UVB irradiation

In this work, UVB irradiation significantly decreased the photochemical efficiency of *R. chrysanthum* leaves expressed as F_v/F_m and ϕ_{PSII} . No statistical difference was observed in the chl content, either total chl or chl *a/b*, and in carotenoid content. Such results align with the finding of UVB inhibition of PSII independent of chl content in leaves exposed to UVB irradiation (Pfundel 2003; Berli *et al.* 2010). In addition, the increased organic acids enhance stress resilience in plants by detoxification of ROS (Farooq *et al.* 2009a, 2009b). Hence, the accumulation of flavonoids and organic acids may protect *R. chrysanthum* plants against UVB deleterious effects (particularly UVB inhibition of PSII in the present study), probably because organic acids contribute to redox balance in photosynthetic membranes by scavenging excessive ROS.

Metabolites related to mitochondrial respiration under UVB irradiation

UVB irradiation increased the intermediates of the arginine biosynthesis and the TCA cycle (Fig. 5; Figs S1 and S2). This suggests that the TCA cycle and arginine biosynthesis in *R. chrysanthum* were enhanced as a protective mechanism

against UVB irradiation. Kim *et al.* (2012, 2018) demonstrated that the metabolites related to the TCA cycle were enhanced in *Melissa officinalis* L. subjected to UVB. According to Kusano *et al.* (2011), the short-term response mainly included rearrangement of primary metabolism, especially increment in the intermediates of the TCA cycle. After that, energy and carbon flux were shifted to aromatic amino acid precursors of the phenylpropanoid pathway as part of long-term protection from UVB irradiation. Similarly, Parida *et al.* (2018) reported that UV affects mitochondrial respiratory pathways, such as the TCA cycle. A complete mechanical model for the changes in *R. chrysanthum* induced by UVB was depicted in Fig. 6.

Conclusion

The present study unravelled the protection mechanism of the plant against UVB irradiation. Accumulation of flavonoids, organic acids, amino acids, fatty acids and enhancement of TCA cycle and arginine biosynthesis may protect *R. chrysanthum* plants against UVB deleterious effects. One possible explanation could be that flavonoids and organic acids are considered to assist the plant in counter excess ROS, and osmotic imbalance caused due to environmental stresses (particularly UVB irradiation in the present study). In addition, increased levels of D-2,3-dihydroxypropanoic acid, maleic acid, fumaric acid and myristoleic acid and decreased levels of 1-linoleoyl-*sn*-monoglyceride in response to UVB irradiation have not been widely reported. They may serve as metabolite biomarkers for screening for greater UVB tolerance in the plant to develop climate-resilient plant varieties.

Supplementary material

Supplementary material is available [online](#).

References

- Abdelrahman M, Burritt DJ, Tran L-SP (2018) The use of metabolomic quantitative trait locus mapping and osmotic adjustment traits for the improvement of crop yields under environmental stresses. *Seminars in Cell & Developmental Biology* **83**, 86–94. doi:10.1016/j.semcdb.2017.06.020
- Ahmad P, Jaleel CA, Salem MA, Nabi G, Sharma S (2010) Roles of enzymatic and nonenzymatic antioxidants in plants during abiotic stress. *Critical Reviews in Biotechnology* **30**, 161–175. doi:10.3109/07388550903524243
- Ahmad P, Tripathi DK, Deshmukh R, Singh VP, Corpas FJ (2019) Revisiting the role of ROS and RNS in plants under changing environment. *Environmental and Experimental Botany* **161**, 1–3. doi:10.1016/j.envexpbot.2019.02.017
- Berli FJ, Moreno D, Piccoli P, Hespanhol-Viana L, Silva MF, Bressan-Smith R, Cavagnaro JB, Bottini R (2010) Abscisic acid is involved in the response of grape (*Vitis vinifera* L.) cv. Malbec leaf tissues to ultraviolet-B radiation by enhancing ultraviolet-absorbing compounds, antioxidant enzymes and membrane sterols. *Plant, Cell & Environment* **33**, 1–10. doi:10.1111/j.1365-3040.2009.02044.x
- Blasco H, Błaszczczyński J, Billaut JC, Nadal-Desbarats L, Pradat PF, Devos D, Moreau C, Andres CR, Emond P, Corcia P, Słowiński R (2015) Comparative analysis of targeted metabolomics: dominance-based rough set approach versus orthogonal partial least square-discriminant analysis. *Journal of Biomedical Informatics* **53**, 291–299. doi:10.1016/j.jbi.2014.12.001
- Casati P, Campi M, Morrow DJ, Fernandes JF, Walbot V (2011) Transcriptomic, proteomic and metabolomic analysis of UV-B signaling in maize. *BMC Genomics* **12**, 321. doi:10.1186/1471-2164-12-321
- Demkura PV, Ballaré CL (2012) UVR8 mediates UV-B-induced *Arabidopsis* defense responses against *Botrytis cinerea* by controlling sinapate accumulation. *Molecular Plant* **5**, 642–652. doi:10.1093/mp/sss025
- Dias MC, Pinto DCGA, Correia C, Moutinho-Pereira J, Oliveira H, Freitas H, Silva AMS, Santos C (2018) UV-B radiation modulates physiology and lipophilic metabolite profile in *Olea europaea*. *Journal of Plant Physiology* **222**, 39–50. doi:10.1016/j.jplph.2018.01.004
- Dias MC, Santos C, Silva S, Pinto DCGA, Silva AM (2020) Physiological and metabolite reconfiguration of *Olea europaea* to cope and recover from a heat or high UV-B shock. *Journal of Agricultural and Food Chemistry* **68**, 11339–11349. doi:10.1021/acs.jafc.0c04719
- Emiliani J, Grotewold E, Falcone F, María L, Casati P (2013) Flavonols protect *Arabidopsis* plants against UV-B deleterious effects. *Molecular Plant* **6**, 1376–1379. doi:10.1093/mp/sst021
- Farooq M, Basra SMA, Wahid A, Ahmad N, Saleem BA (2009a) Improving the drought tolerance in rice (*Oryza sativa* L.) by exogenous application of salicylic acid. *Journal of Agronomy and Crop Science* **195**, 237–246. doi:10.1111/j.1439-037X.2009.00365.x
- Farooq M, Wahid A, Ito O, Lee D-J, Siddique KHM (2009b) Advances in drought resistance of rice. *Critical Reviews in Plant Sciences* **28**, 199–217. doi:10.1080/07352680902952173
- Fasano R, Gonzalez N, Tosco A, Dal Piaz F, Docimo T, Serrano R, Grillo S, Leone A, Inzé D (2014) Role of *Arabidopsis* UV RESISTANCE LOCUS 8 in plant growth reduction under osmotic stress and low levels of UV-B. *Molecular Plant* **7**(5), 773–791. doi:10.1093/mp/ssu002
- Guyon I, Elisseeff A (2003) An introduction to variable and feature selection. *Journal of Machine Learning Research* **3**, 1157–1182. doi:10.1162/153244303322753616
- Hamid A, Singh S, Agrawal M, Agrawal SB (2018) *Heteropogon contortus* BL-1 (Pilli Grass) and elevated UV-B radiation: the role of growth, physiological and biochemical traits in determining forage productivity and quality. *Photochemistry and Photobiology* **95**, 572–580. doi:10.1111/php.12990
- Hamid A, Singh S, Agrawal M, Agrawal SB (2020) Effects of plant age on performance of the tropical perennial fodder grass, *Cenchrus ciliaris* L. subjected to elevated ultraviolet-B radiation. *Plant Biology* **22**(5), 805–812. doi:10.1111/plb.13116
- Hong J, Yang L, Zhang D, Shi J (2016) Plant metabolomics: an indispensable system biology tool for plant science. *International Journal of Molecular Sciences* **17**, 767. doi:10.3390/ijms17060767
- Hugly S, Kunst L, Browse J, Somerville C (1989) Enhanced thermal tolerance of photosynthesis and altered chloroplast ultrastructure in a mutant *Arabidopsis* deficient in lipid peroxidation. *Plant Physiology* **90**, 1134–1142. doi:10.1007/s00018-012-1091-5
- Jan S, Alyemni MN, Wijaya L, Alam, P, Siddique KH, Ahmad P (2018) Interactive effect of 24-epibrassinolide and silicon alleviates cadmium stress via the modulation of antioxidant defense and glyoxalase systems and macronutrient content in *Pisum sativum* L. seedlings. *BMC Plant Biology* **18**, 146. doi:10.1186/s12870-018-1359-5
- Kasote DM, Katyare SS, Hegde MV, Bae H (2015) Significance of antioxidant potential of plants and its relevance to therapeutic applications. *International Journal of Biological Sciences* **11**, 982–991. doi:10.7150/ijbs.12096
- Kaya C, Okant M, Ugurlar F, Alyemni MN, Ashraf M, Ahmad P (2019) Melatonin-mediated nitric oxide improves tolerance to cadmium toxicity by reducing oxidative stress in wheat plants. *Chemosphere* **225**, 627–638. doi:10.1016/j.chemosphere.2019.03.026
- Kim S, Yun EJ, Hossain MA, Lee H, Kim KH (2012) Global profiling of ultraviolet-induced metabolic disruption in *Melissa officinalis* by using gas chromatography-mass spectrometry. *Analytical and Bioanalytical Chemistry* **404**, 553–562. doi:10.1007/s00216-012-6142-0

- Kim S, Lee H, Kim KH (2018) Metabolomic elucidation of recovery of *Melissa officinalis* from UV-B irradiation stress. *Industrial Crops and Products* **121**, 428–433. doi:10.1016/j.indcrop.2018.05.002
- Knox PP, Lukashev EP, Gorokhov VV, Grishanova NP, Paschenko VZ (2019) Hybrid complexes of photosynthetic reaction centers and quantum dots in various matrices: resistance to UV irradiation and heating. *Photosynthesis Research* **139**, 295–305. doi:10.1007/s11120-018-0529-5
- Kohli SK, Khanna K, Bhardwaj R, Abd Allah EF, Ahmad P, Corpas FJ (2019) Assessment of subcellular ROS and NO metabolism in higher plants: multifunctional signaling molecules. *Antioxidants* **8**, 641. doi:10.3390/antiox8120641
- Kramer GF, Norman HA, Krizek DT, Mirecki RM (1991) Influence of UV-B radiation on polyamines, lipid peroxidation and membrane lipids in cucumber. *Phytochemistry* **30**, 2101–2108. doi:10.1016/0031-9422(91)83595-C
- Kreslavski VD, Shmarev AN, Lyubimov VY, Semenova GA, Zharmukhamedov SK, Shirshikova GN, Khudyakova AY, Allakhverdiev SI (2018) Response of photosynthetic apparatus in *Arabidopsis thaliana* L. mutant deficient in phytochrome A and B to UV-B. *Photosynthetica* **56**, 418–426. doi:10.1007/s11099-017-0754-8
- Kusano M, Tohge T, Fukushima A, Kobayashi M, Hayashi N, Otsuki H, Kawashima M, Matsuda F, Niida R (2011) Metabolomics reveals comprehensive reprogramming involving two independent metabolic responses of *Arabidopsis* to UV-B light. *The Plant Journal* **67**, 354–369. doi:10.1111/j.1365-3113X.2011.04599.x
- Lyu J, Wang C, Liang DY, Liu L, Pandey LK, Xu HW, Zhou XF (2019) Sensitivity of wild and domesticated *Rhododendron chrysanthum* to different light regime (UVA, UVB, and PAR). *Photosynthetica* **57**, 841–849. doi:10.32615/ps.2019.098
- Machado F, Dias MC, de Pinho PG, Araújo AM, Pinto D, Silva A, Correia C, Moutinho-Pereira J, Santos C (2017) Photosynthetic performance and volatile organic compounds profile in *Eucalyptus globulus* after UVB radiation. *Environmental and Experimental Botany* **140**, 141–149. doi:10.1016/j.envexpbot.2017.05.008
- Moorthy K, Kathiresan P (1998) UV-B induced alterations in composition of thylakoid membrane and amino acids in leaves of *Rhizophora apiculata* Blume. *Photosynthetica* **35**, 321–328. doi:10.1023/A:1006947831556
- Obata T, Fernie AR (2012) The use of metabolomics to dissect plant responses to abiotic stresses. *Cellular and Molecular Life Sciences* **69**, 3225–3243. doi:10.1007/s00018-012-1091-5
- Parida AK, Panda A, Rangani J (2018) Metabolomics-guided elucidation of abiotic stress tolerance mechanisms in plants. In 'Plant metabolites and regulation under environmental stress'. (Eds P Ahmad, MA Ahanger, VP Singh, DK Tripathi, P Alam, MN Alyemeni) pp. 89–131. (Academic Press: London, UK) doi:10.1016/B978-0-12-812689-9.00005-4
- Peng M, Shahzad R, Gul A, Subthain H, Shen S, Lei L, Zheng Z, Zhou J, Lu D, Wang S, Nishawy E, Liu X, Tohge T, Fernie AR, Luo J (2017) Differentially evolved glucosyltransferases determine natural variation of rice flavone accumulation and UV-tolerance. *Nature Communications* **8**, 1975. doi:10.1038/s41467-017-02168-x
- Pföndel EE (2003) Action of UV and visible radiation on chlorophyll fluorescence from dark-adapted grape leaves (*Vitis vinifera* L.). *Photosynthesis Research* **75**, 29–39. doi:10.1023/A:1022486925516
- Popescu R, Kopp B (2013) The genus *Rhododendron*: an ethnopharmacological and toxicological review. *Journal of Ethnopharmacology* **147**, 42–62. doi:10.1016/j.jep.2013.02.022
- Qiu Y, Cai G, Zhou B, Li D, Zhao A, Xie G, Li H, Cai S, Xie D, Huang C, Ge W, Zhou Z, Xu LX, Jia W, Zheng S, Yen Y, Jia W (2014) A distinct metabolic signature of human colorectal cancer with prognostic potential. *Clinical Cancer Research* **20**, 2136–2146. doi:10.1158/1078-0432.CCR-13-1939
- Rama PG, Vinutha T (2019) Metabolomic profiling of plants to understand reasons for plant stress resilience to abiotic stress. In 'Recent approaches in omics for plant resilience to climate change'. (Ed. S Wani) pp. 57–74. (Springer: Cham, Switzerland) doi:10.1007/978-3-030-21687-0_3
- Rostami-Hodjegan A, Nurminen S, Jackson PR, Tucker GT (1996) Caffeine urinary metabolite ratios as markers of enzyme activity: a theoretical assessment. *Pharmacogenetics* **6**, 121–149. doi:10.1097/00008571-199604000-00001
- Rostami-Hodjegan A, Kroemer HK, Tucker GT (1999) In-vivo indices of enzyme activity: the effect of renal impairment on the assessment of CYP2D6 activity. *Pharmacogenetics* **9**, 277–286. doi:10.1097/00008571-199906000-00002
- Takshak S, Agrawal SB (2019) Defense potential of secondary metabolites in medicinal plants under UV-B stress. *Journal of Photochemistry and Photobiology B: Biology* **193**, 51–88. doi:10.1016/j.jphotobiol.2019.02.002
- Tang H, Zhang X, Gong B, Yan Y, Shi Q (2020) Proteomics and metabolomics analysis of tomato fruit at different maturity stages and under salt treatment. *Food Chemistry* **311**, 126009. doi:10.1016/j.foodchem.2019.126009
- Xie Z, Wang J, Wang W, Wang Y, Xu J, Li Z, Zhao X, Fu B (2021) Integrated analysis of the transcriptome and metabolome revealed the molecular mechanisms underlying the enhanced salt tolerance of rice due to the application of exogenous melatonin. *Frontiers in Plant Science* **11**, 618680. doi:10.3389/fpls.2020.618680
- Yadav A, Lingwan M, Yadukrishnan P, Masakapalli SK, Datta S (2019) BBX31 promotes hypocotyl growth, primary root elongation and UV-B tolerance in *Arabidopsis*. *Plant Signaling & Behavior* **14**, e1588672. doi:10.1080/15592324.2019.1588672
- Zhou X, Chen S, Wu H, Yang Y, Xu H (2017) Biochemical and proteomics analyses of antioxidant enzymes reveal the potential stress tolerance in *Rhododendron chrysanthum* Pall. *Biology Direct* **12**, 10. doi:10.1186/s13062-017-0181-6

Data availability. The datasets used and/or analysed during the current study are available from the corresponding author on reasonable request.

Conflicts of interest. The authors declare no conflicts of interest.

Declaration of funding. This work was supported by the Department of Finance of Jilin Province, China (grant numbers 2018-1).

Acknowledgements. We thank Hangzhou PTM Biolabs Inc. for excellent technical assistance.

Author affiliations

^AFaculty of Jilin Provincial Key Laboratory of Plant Spectral Regions Science and Green Production, Jilin Normal University, Siping 136000, China.

^BFaculty of Biological Science and Technology, Baotou Teachers' College, Baotou 014030, China.

^CFaculty of Siping Central People's Hospital, Siping 136000, China.